Evidence of momentum-dependent hybridization in $Ce_2Co_{0.8}Si_{3.2}$

P. Starowicz,[1,*] R. Kurleto,[1] J. Goraus,[2] H. Schwab,[3,4] M. Szlawska,[5] F. Forster,[3,4] A. Szytuła,[1] I. Vobornik,[6] D. Kaczorowski,[5] and F. Reinert[3,4]

[1]*M. Smoluchowski Institute of Physics, Jagiellonian University, Reymonta 4, 30-059 Kraków, Poland*
[2]*Institute of Physics, University of Silesia, Uniwersytecka 4, 40-007 Katowice, Poland*
[3]*Universität Würzburg, Experimentelle Physik VII, Am Hubland, D-97074 Würzburg, Germany*
[4]*Karlsruher Institut für Technologie KIT, Gemeinschaftslabor für Nanoanalytik, D-76021 Karlsruhe, Germany*
[5]*Institute of Low Temperature and Structure Research, Polish Academy of Sciences, P.O. Box 1410, 50-950 Wrocław, Poland*
[6]*CNR-IOM, TASC Laboratory, SS 14, km 163.5, I-34149 Trieste, Italy*

(Received 29 October 2013; revised manuscript received 23 January 2014; published 21 March 2014)

We studied the electronic structure of the Kondo lattice system $Ce_2Co_{0.8}Si_{3.2}$ by angle-resolved photoemission spectroscopy. The spectra obtained below the coherence temperature consist of a Kondo resonance, its spin-orbit partner, and a number of dispersing bands. The quasiparticle weight related to the Kondo peak depends strongly on Fermi vectors associated with bulk bands. This indicates a highly anisotropic hybridization between conduction-band and $4f$ electrons—V_{cf} in $Ce_2Co_{0.8}Si_{3.2}$.

DOI: 10.1103/PhysRevB.89.115122 PACS number(s): 71.27.+a, 71.20.Eh, 74.25.Jb, 75.30.Mb

I. INTRODUCTION

Cerium intermetallics are rich in exciting phenomena due to various manifestations of the hybridization between a conduction band and $4f$ electrons (V_{cf}) based on the Kondo interaction [1,2]. Among the most peculiar effects one may list the formation of heavy fermions, unconventional superconductivity, quantum critical phenomena, and non-Fermi liquid behavior. Microscopic models for heavy-fermion (HF) systems assume very often that the strength of V_{cf} hybridization is momentum independent [3]. On the other hand, there are theoretical considerations [3–5] indicating a strong momentum dependence of V_{cf} with possible maxima and nodes. This complex variation of the V_{cf} amplitude is expected to result from the symmetry of f electrons, which participate in the formation of the Kondo singlet. Therefore, the issue of V_{cf} anisotropy deserves more attention in the experimental investigation of f-electron systems.

A typical spectroscopic manifestation of the Kondo effect is the Abrikosov-Suhl resonance, also called the Kondo resonance (KR), which is a narrow high-intensity peak in the spectral function located close to the Fermi energy (E_F) [6,7]. In case of Ce-based systems, angle-resolved photoemission spectroscopy (ARPES) was able to determine a k-vector-dependent intensity variation of the KR [8–11]. It was reported that the increased KR intensity is found at normal emission [10] or at k vectors related to bands crossing E_F (Fermi vectors) [11]. Recently, it was shown for $CeCoIn_5$ [12] that the f-electron peak intensity depends considerably on a band crossing E_F, which was interpreted in terms of an anisotropic V_{cf}. Optical spectroscopy [13] also reveals anisotropic hybridization for the Ce-115 compound. Another effect of the $4f$–conduction band hybridization is KR dispersion or more precisely heavy quasiparticle dispersion, which has also been found in Ce systems [9,14–17]. Nevertheless, a complete image of momentum-dependent hybridization strength V_{cf} with the occurrence of eventual nodes predicted by theory [3–5] remains a challenge for an experiment so far.

The object of our investigations, $Ce_2Co_{0.8}Si_{3.2}$, crystallizes with a derivative of the hexagonal AlB_2-type structure with the $P6/mmm$ space group [18]. As established from detailed magnetic susceptibility, electrical resistivity, and heat capacity measurements of single-crystalline specimens, $Ce_2Co_{0.8}Si_{3.2}$ does not order magnetically down to 0.4 K. Its physical behavior at low temperatures is governed by strong f-ligand hybridization, leading to enhanced electronic contribution to the specific heat [$C/T = 200$ mJ/(mol$_{Ce}$K^2) at 0.4 K] and Kondo-like temperature variations of the electrical resistivity with the characteristic temperature T_K of about 50 K [18]. The $\rho(T)$ dependencies are dominated by broad maxima near 80 K, which manifest a crossover from incoherent to coherent Kondo regime. Most interestingly, below 10 K, all the bulk characteristics of $Ce_2Co_{0.8}Si_{3.2}$ show non-Fermi-liquid (NFL) features that are compatible with theoretical predictions for Griffiths phases. These should be related to a disorder in the Ce-Si sublattice found recently [18]. So far, photoemission spectroscopy (PES) studies performed on Ce_2CoSi_3 polycrystals delivered only angle-integrated spectra showing a KR [19,20].

In this paper, we present ARPES studies of the Kondo lattice $Ce_2Co_{0.8}Si_{3.2}$ system. The spectra consist of dispersions originating from surface and bulk states and a Kondo peak related mainly to bulk states. A specific k-vector dependence of KR indicates that certain bulk bands cross E_F with much higher quasiparticle weight than others. These results point to a momentum- and/or band-dependent anisotropic V_{cf} hybridization in $Ce_2Co_{0.8}Si_{3.2}$.

II. EXPERIMENT

Single crystals of $Ce_2Co_{0.8}Si_{3.2}$ have been grown by the Czochralski method and characterized as described elsewhere [18]. The ARPES experiment was conducted at the APE beam line of the Elettra synchrotron [21] with an SES2002 electron spectrometer. Prior to the photoemission studies the crystals

*pawel.starowicz@uj.edu.pl

were oriented with a Laue method. Subsequently, they were cleaved at a pressure of 2×10^{-11} mbar, exposing flat surfaces along the $(10\bar{1}0)$ crystallographic plane. The measurements were carried out with linearly polarized radiation, typically at a temperature of 25 K. The energy and wave-vector resolution was fixed to 18 meV and 0.01 Å^{-1}, respectively. The Fermi energy was determined regularly on evaporated gold. Band-structure calculations were performed for stoichiometric Ce_2CoSi_3 using the scalar relativistic version of the full-potential local-orbital (FPLO) code [22] with the Perdew-Wang [23] exchange-correlation potential. Additional correlations within the local spin-density approximation (LSDA) + U approach were accomplished employing the around-mean-field scheme [24]. An irreducible wedge of the Brillouin zone comprised 133 points.

III. RESULTS AND DISCUSSION

A. Valence band studied with PES and FPLO

The valence band of $Ce_2Co_{0.8}Si_{3.2}$ was investigated by means of photoemission spectroscopy with the photon energies ($h\nu$) corresponding to lower ($h\nu = 25$ eV) and higher ($h\nu = 40$ eV) photoionization cross section for Ce $4f$ electrons [25]. The spectra obtained by integrating ARPES data for $h\nu = 40$ eV and $h\nu = 25$ eV are shown in Fig. 1. Usually, one calculates the difference of the spectra corresponding to these energies to approximate a contribution from $4f$ electrons. However, in the case of $Ce_2Co_{0.8}Si_{3.2}$ the photoionization cross section for Co $3d$ electrons almost doubles for the excitation energy increase from 25 to 40 eV according to the estimates for free atoms [25]. Hence, the contribution from both orbitals, Ce $4f$ and Co $3d$, is estimated by such a subtraction.

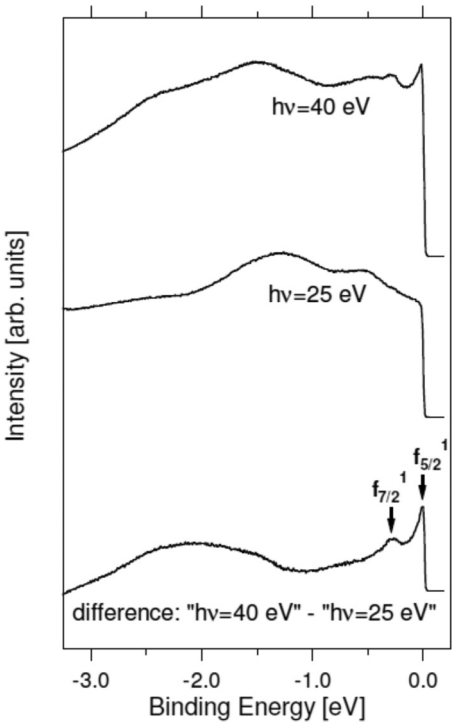

FIG. 1. Photoemission spectra obtained with photon energies of $h\nu = 40$ and 25 eV resulting from angle integration of the ARPES data collected along the $\bar{\Gamma}$-$\bar{Y}$ direction of $Ce_2Co_{0.8}Si_{3.2}$ and their difference.

The peaks of the well-screened $f^1_{5/2}$ and $f^1_{7/2}$ final states (Fig. 1) indicate a high hybridization between $4f$ and conduction-band electrons. The characteristic tail of the Kondo peak $f^1_{5/2}$ is located near E_F and its spin-orbit partner $f^1_{7/2}$ at 275 meV. The broad peak at ~2 eV cannot solely be attributed to the weakly screened f^0 final state. This is because the ARPES data (Fig. 2) reveal high-intensity dispersing peaks near this energy, which cannot originate from highly localized and weakly hybridized f electrons. Thus, a large part of the spectral weight at ~2 eV should be attributed to Co $3d$ electrons. Density of states (DOS) obtained theoretically (not shown) by means of the FPLO method with LSDA approach indicates that Si $3p$, Co $3d$, and Ce $4f$ dominate the valence band. The contribution from Si $3p$ to the photoemission spectra is less significant due to a very low photoionization cross section at $h\nu = 25$ and 40 eV.

Further insight into the electronic structure of $Ce_2Co_{0.8}Si_{3.2}$ is given by band mapping with ARPES. The path scanned in the reciprocal space is shown as a green dashed curve inside the three-dimensional (3D) Brillouin zone (BZ) [Fig. 2(a)]. This curve is part of a large circle in the Γ-A-L-M plane, for which the perpendicular to the surface component of the wave vector ($k_\perp$) is unknown. For surface states the problem is reduced to two dimensions and the band structure is scanned along $\bar{\Gamma}$-$\bar{Y}$, which is drawn with a green dashed straight line in the surface Brillouin zone (SBZ). As the considered ARPES data do not deliver any information about the real value of $k_\perp$, both two-dimensional and 3D bands are described in the SBZ for simplicity.

The measurements were performed with $h\nu = 40$ eV at a temperature of 25 K, which is below the coherence temperature estimated to be $T_{coh} \sim 80$ K. KR and the spin-orbit partner are not dispersing but vary in intensity. The other peaks reveal dispersions. In particular, α and β bands (Fig. 2) clearly cross E_F. The electron pocket (α) observed around the $\bar{\Gamma}$ points is more shallow near $k_\parallel = 0$ than at $k_\parallel \sim 1.5$ Å^{-1}. The locations in the reciprocal space scanned by ARPES for $k_\parallel = 0$ and $k_\parallel = 1.5$ Å^{-1} do not share the same out-of-plane component of the wave vector $k_\perp$ according to the free-electron final-state model [26]. Hence, 3D states exhibit different dispersions for the equivalent $k_\parallel$ but different $k_\perp$ in neighboring BZs. Therefore, the α pocket is considered to be a 3D band of bulk origin.

The β band crossing E_F at $\bar{\Gamma}$ is well visible at $k_\parallel \sim 1.5$ Å^{-1} in contrast to $k_\parallel \sim 0$ Å^{-1}. This parabolic band exhibits the same dispersion in both BZs and is therefore regarded as a surface state. It has the highest spectral intensity of all features in the spectrum, which is expected for surface states at the photon energy of $h\nu = 40$ eV. This is due to the very small mean free path of electrons for this energy [27]. The difference in the intensity at $k_\parallel \sim 1.5$ Å^{-1} and $k_\parallel \sim 0$ Å^{-1} may be attributed to matrix element effects, which favor certain bands with a higher photoemission cross section, depending on the geometry of the experiment, k vector, and probed BZ. This may result in suppression or disappearance of particular bands. In fact, the β band loses intensity when approaching $k_\parallel = 0$ Å^{-1}. At this wave vector the experiment is realized in

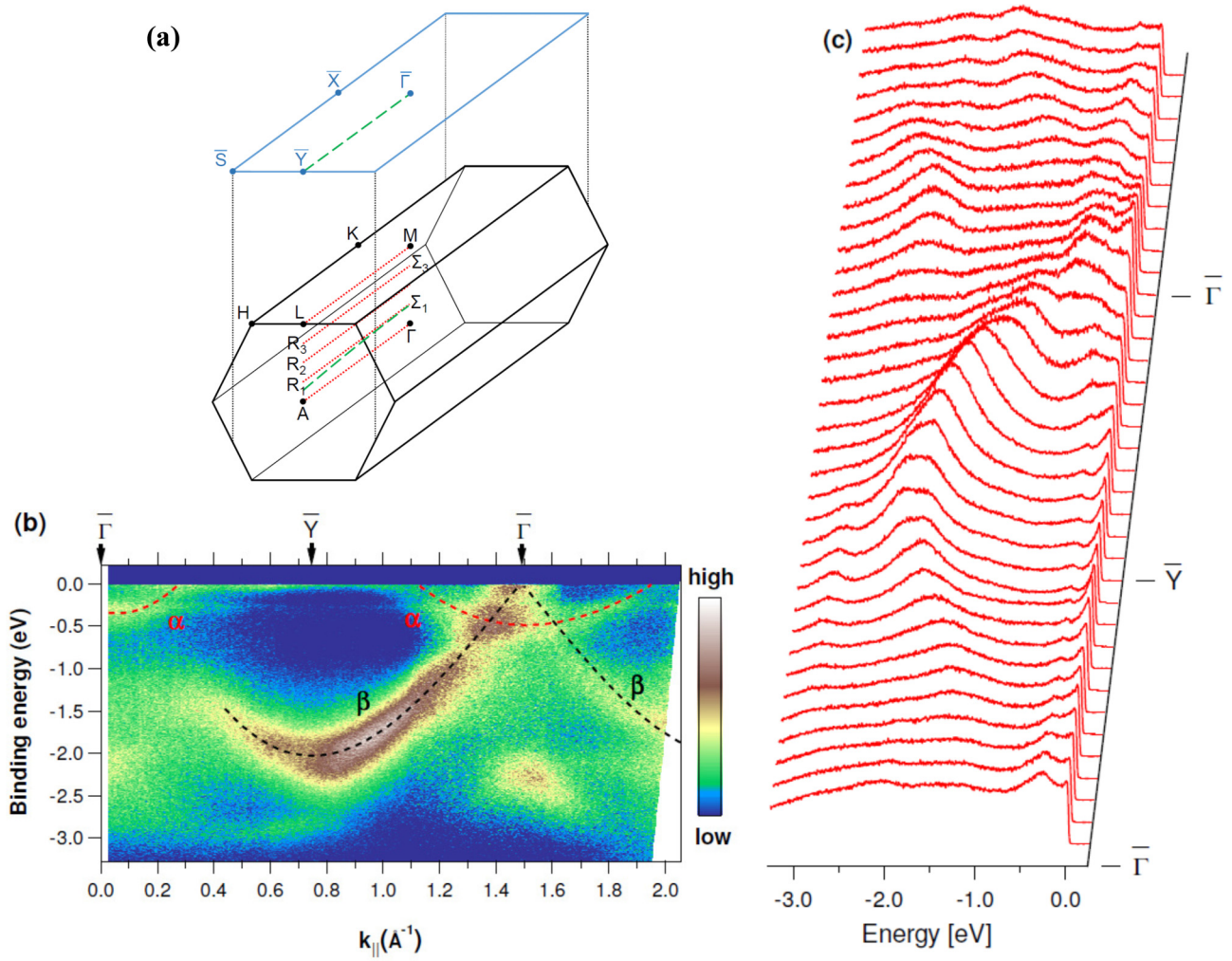

FIG. 2. (Color online) (a) Three-dimensional Brillouin zone (black) and surface Brillouin zone (blue) along $(10\bar{1}0)$ plane for $Ce_2Co_{0.8}Si_{3.2}$ with marked high-symmetry points. Dashed (green) line indicates a possible path in the reciprocal space along which ARPES spectra were collected. Dotted (red) lines represent paths Γ-A, Σ_1-R_1, Σ_2-R_2, Σ_3-R_3, and M-L used for band-structure calculations. (b) ARPES spectra for $Ce_2Co_{0.8}Si_{3.2}$ obtained with the photon energy $h\nu = 40$ eV along the $\bar{\Gamma}$-$\bar{Y}$ direction shown as intensity map and (c) energy distribution curves. Dashed lines are guides to the eye indicating α and β bands. The temperature of the sample was 25 K.

a pure π polarization, which excludes bands with odd parity with respect to the experimental mirror plane. Due to this we cannot conclude whether this band crosses E_F near $k_\parallel = 0$ Å^{-1} or bends back to higher energies.

Band-structure calculations using the FPLO method (Fig. 3) are helpful for a further interpretation of the ARPES results. Theoretical dispersions for bulk Ce_2CoSi_3 are drawn along a conventional path in the reciprocal space [Fig. 3(a)] and for a set of directions parallel to Γ-A [Fig. 3(b)]. The real path for the ARPES studies should be located close to one of the latter directions [see also Fig. 2(a)]. To consider different strengths of correlation the calculations were performed with the Ce $4f$ correlation parameters $U_{4f} = 0$ (not shown) and $U_{4f} = 6$ eV. The calculations yield more bands than observed in the experiment. A certain number of them cannot be seen because of unfavorable matrix elements. The electron pocket α found experimentally near Γ has its counterpart in the calculations for $U_{4f} = 6$ eV along Γ-A and Σ_1-R_1. It reaches higher binding energy along Γ-A and is a 3D state. On the other hand, the exact β dispersion is not found in the calculations. This confirms the surface-state origin of this band. The other bands recorded with a weaker intensity (Fig. 2) have corresponding dispersions in the calculations with both $U_{4f} = 0$ and 6 eV. The theoretical band structure consists of two components related to opposite spin direction. This is due to a magnetic ground state predicted by calculations, which is, however, not found in the experiment. This discrepancy can be explained by the fact that in the calculations the total energy difference between magnetic and nonmagnetic ground state is so low that even at low temperatures the thermal excitations would destroy long-range magnetic order. Moreover, the Kondo scattering present in $Ce_2Co_{0.8}Si_{3.2}$ should screen magnetic interactions.

B. $k_\parallel$-dependence of Kondo resonance intensity

ARPES data provide a direct evidence of KR intensity variation with $k_\parallel$, while its dispersion is not found at $T = 25$ K,

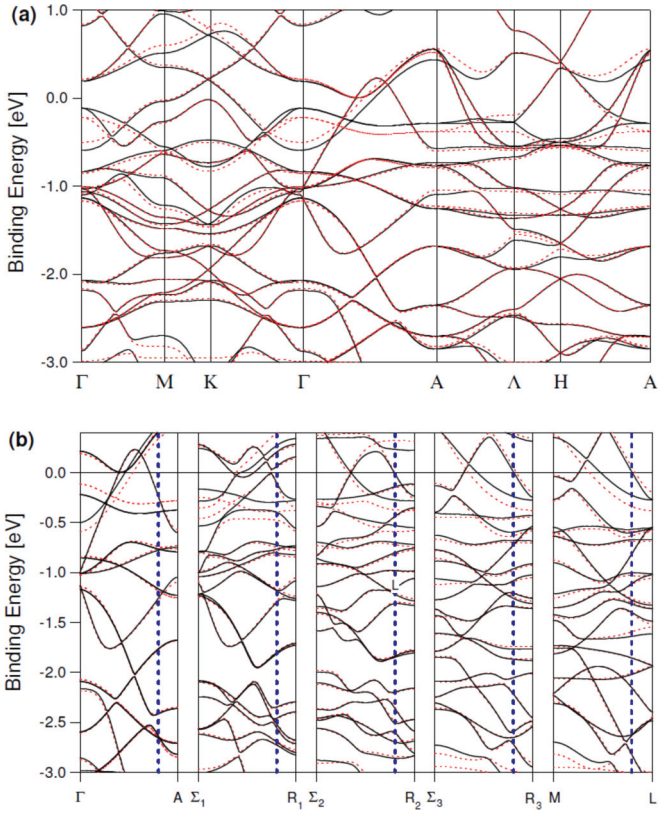

FIG. 3. (Color online) Theoretical dispersions obtained for bulk Ce_2CoSi_3 by means of FPLO with LSDA + U approximation for $U_{4f} = 6$ eV along (a) a standard path connecting high-symmetry points and (b) for the directions parallel to Γ-A. The high-symmetry points are defined in Fig. 2(a). The vertical dashed line denotes $k_\parallel = 0.6$ Å^{-1} with the highest KR. Solid (black) and dashed (red) lines show dispersions corresponding to spin-up and spin-down directions, respectively.

a temperature well below the coherence temperature of the Kondo lattice, $T_{coh} \sim 80$ K. Energy distribution curves (EDCs) for exemplary k vectors from Figs. 2(b) and 2(c) are shown in Fig. 4. The height of the KR (blue arrow) was estimated with respect to the background located between the KR and the spin-orbit splitting peak after proper normalization of the EDCs. The first surprising fact is that the Kondo peak intensity is not directly correlated with the Fermi wave vectors found in the same experiment. E_F crossings at $k_\parallel = 0.3$, 1.1, and 1.9 Å^{-1}, which are related to the most prominent bulk state, namely the α electron pocket, exhibit a relatively low intensity Kondo peak. On the other hand, the highest-intensity KR is found around $k_\parallel = 0.6$ Å^{-1}, where bands crossing the Fermi energy are not directly observed. The ARPES measurements were performed a few times to exclude the effects of surface quality, and KR intensity dependence on k is reproducible.

It is known that the KR may have a much higher intensity than its parent band, which crosses E_F [11]. Therefore, it is possible that the band responsible for the high KR intensity is not visible. Bulk $4f$ electrons are known for a stronger hybridization with the valence-band electrons as compared to surface states [28] and they may form a high-intensity KR. Hence, the large KR should be assigned to a band, which is not seen in the experiment and should be a bulk state. This experimental material points to the main conclusion of this paper, namely a large variation of the Kondo peak intensity along the Fermi surface (FS). The KR is much higher for a weak-intensity band at $k_\parallel = 0.6$ Å^{-1} than for the well-visible α pocket. Thus, taking into account band intensities, one may conclude that the real KR height variation is even much larger. It is also noteworthy that the intensity of the KR is lower for $k_\parallel = 0.9$ Å^{-1} than for $k_\parallel = 0.6$ Å^{-1}, wave vectors that are equivalent in the SBZ. Due to the circular path of the ARPES experiment mentioned before, these $k_\parallel$ vectors correspond to different values of $k_\perp$ and thus different locations in the BZ. Inequality of KR height in these places is consistent with the 3D nature of the related states.

In order to assign the highest-intensity KR to a particular band, the results of band-structure calculations are shown along Γ-A, M-L, and the paths in between for LSDA + U approximation with $U_{4f} = 6$ eV [Fig. 3(b)]. The wave vector 0.6 Å^{-1} corresponding to the highest KR is highlighted with a dashed line. Actually, an E_F crossing at 0.6 Å^{-1} appears for almost all considered paths parallel to Γ-A. It should be stressed that in the case of each considered path there are more E_F crossings but the highest intensity KR is observed only at the unique wave vector in ARPES. The KR absence may also be explained by unfavorable photoionization cross section for certain bands. Nevertheless, the main thesis is based on the experimental spectra, namely on the comparison of KR height for the α band and at $k_\parallel = 0.6$ Å^{-1}.

$Ce_2Co_{0.8}Si_{3.2}$ was investigated in the coherent state. Although the f-state dispersion was not found directly in the experiment, we assume that f-electron-related quasiparticles are present. The high-intensity KR peak should refer to a high quasiparticle spectral weight, $Z(k)$, for a given momentum. Its considerable variation along the FS indicates also the momentum dependence of V_{cf}. Such a situation was proposed in the theoretical considerations for a Ce-based cubic system [5]. These predicted strongly anisotropic V_{cf} resulting in a variation of $Z(k)$ along the Brillouin zone. In the cited report a high quasiparticle weight [$Z(k) \sim 1$] was found only in very small areas of the FS along [001] and equivalent symmetry directions. According to the predictions, these regions can be easily missed by ARPES due to their very limited size in k space. Although similar calculations are not realized for $Ce_2Co_{0.8}Si_{3.2}$, our ARPES results support the theoretical predictions qualitatively giving the evidence of strongly anisotropic V_{cf} in the $Ce_2Co_{0.8}Si_{3.2}$ system.

IV. CONCLUSION

We investigated the band structure of $Ce_2Co_{0.8}Si_{3.2}$ by means of ARPES and FPLO calculations with the LSDA + U approach. Out of a larger number of bands theoretically predicted for bulk Ce_2CoSi_3 only some can be seen in the experiment. ARPES data reveal a bulk electron pocket near the Γ point (α), which is found in the calculations with $U_{4f} = 6$ eV. The band β exhibiting the highest intensity is

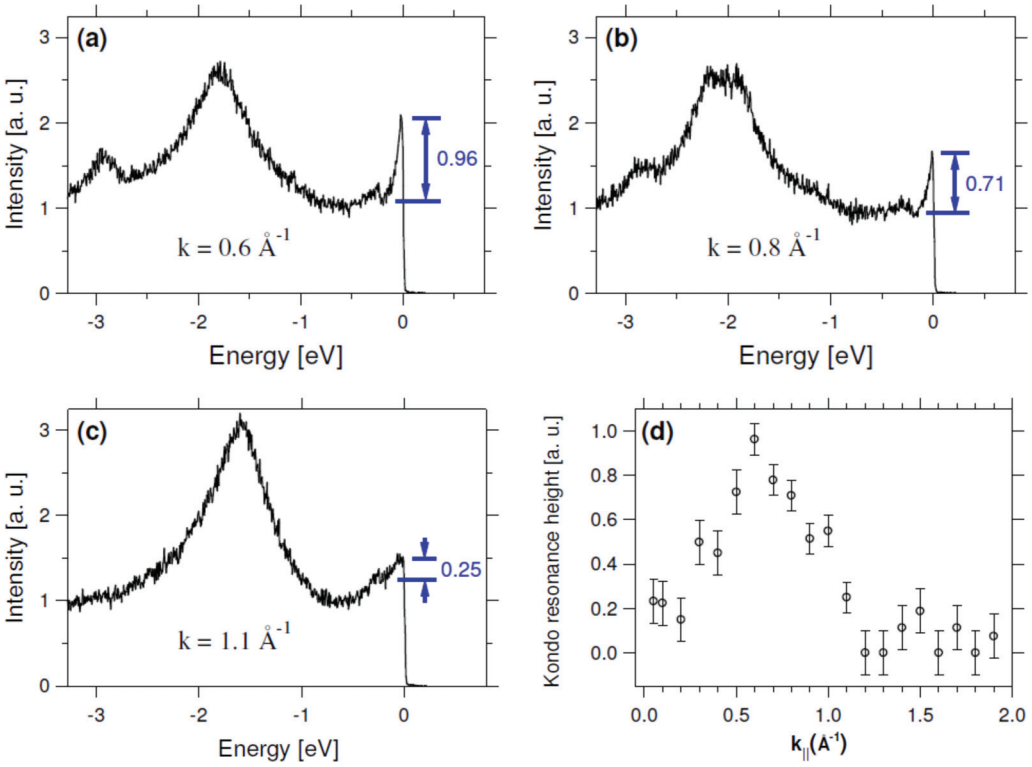

FIG. 4. (Color online) Energy distribution curves extracted from the ARPES data ($h\nu = 40$ eV) in Fig. 2 shown for (a) $k_{\|} = 0.6$ Å^{-1}, (b) $k_{\|} = 0.8$ Å^{-1}, and (c) $k_{\|} = 1.1$ Å^{-1} with determined KR height. (d) KR height dependence on $k_{\|}$.

interpreted as a surface state. The main contributions from Ce $4f$ electrons to the photoemission spectra are the KR at E_F associated with the $f^1_{5/2}$ final state and the peak related to the $f^1_{7/2}$ final state observed at 275 meV. Both peaks are nondispersing but their intensity varies as a function of the wave vector. In particular, a large maximum of KR is attributed to a specific Fermi vector of a bulk band, whereas the other observed bands from the bulk or the surface are characterized with a medium or low quasiparticle weight at Fermi vectors. This represents the ARPES evidence of a momentum-dependent hybridization between Ce $4f$ and conduction-band electrons in $Ce_2Co_{0.8}Si_{3.2}$.

ACKNOWLEDGMENTS

This work has been supported by the Ministry of Science and Higher Education in Poland within Grant No. N N202 201 039. A part of the measurements was carried out with equipment purchased thanks to the European Regional Development Fund in the framework of the Polish Innovation Economy Operational Program (Contract No. POIG.02.01.00-12-023/08). H.S., F.F., and F.R. acknowledge the support by the DFG through FOR1162. We acknowledge technical support by F. Salvador (CNR-IOM). J.G. acknowledges the financial support from the National Science Centre (NCN), on the basis of Decision No. DEC-2012/07/B/ST3/03027.

[1] G. R. Stewart, Rev. Mod. Phys. **56**, 755 (1984).
[2] A. C. Hewson, *The Kondo Problem to Heavy Fermions* (Cambridge University Press, Cambridge, 1993).
[3] H. Weber and M. Vojta, Phys. Rev. B **77**, 125118 (2008).
[4] J. H. Shim, K. Haule, and G. Kotliar, Science **318**, 1615 (2007).
[5] P. Ghaemi, T. Senthil, and P. Coleman, Phys. Rev. B **77**, 245108 (2008).
[6] D. Malterre, M. Grioni, and Y. Baer, Adv. Phys. **45**, 299 (1996).
[7] J. W. Allen, J. Phys. Soc. Jpn. **74**, 34 (2005).
[8] A. B. Andrews, J. J. Joyce, A. J. Arko, J. D. Thompson, J. Tang, J. M. Lawrence, and J. C. Hemminger, Phys. Rev. B **51**, 3277 (1995).
[9] A. B. Andrews, J. J. Joyce, A. J. Arko, Z. Fisk, and P. S. Riseborough, Phys. Rev. B **53**, 3317 (1996).
[10] M. Garnier, D. Purdie, K. Breuer, M. Hengsberger, and Y. Baer, Phys. Rev. B **56**, R11399 (1997).
[11] S. Danzenbächer, Yu. Kucherenko, M. Heber, D. V. Vyalikh, S. L. Molodtsov, V. D. P. Servedio, and C. Laubschat, Phys. Rev. B **72**, 033104 (2005).
[12] A. Koitzsch, T. K. Kim, U. Treske, M. Knupfer, B. Büchner, M. Richter, I. Opahle, R. Follath, E. D. Bauer, and J. L. Sarrao, Phys. Rev. B **88**, 035124 (2013).
[13] K. S. Burch, S. V. Dordevic, F. P. Mena, A. B. Kuzmenko, D. van der Marel, J. L. Sarrao, J. R. Jeffries, E. D. Bauer, M. B. Maple, and D. N. Basov, Phys. Rev. B **75**, 054523 (2007).

[14] S.-I. Fujimori *et al*., Phys. Rev. B **73**, 224517 (2006).
[15] H. J. Im, T. Ito, H.-D. Kim, S. Kimura, K. E. Lee, J. B. Hong, Y. S. Kwon, A. Yasui, and H. Yamagami, Phys. Rev. Lett. **100**, 176402 (2008).
[16] A. Koitzsch, S. V. Borisenko, D. Inosov, J. Geck, V. B. Zabolotnyy, H. Shiozawa, M. Knupfer, J. Fink, B. Büchner, E. D. Bauer, J. L. Sarrao, and R. Follath, Phys. Rev. B **77**, 155128 (2008).
[17] M. Klein, A. Nuber, H. Schwab, C. Albers, N. Tobita, M. Higashiguchi, J. Jiang, S. Fukuda, K. Tanaka, K. Shimada, M. Mulazzi, F. F. Assaad, and F. Reinert, Phys. Rev. Lett. **106**, 186407 (2011).
[18] M. Szlawska and D. Kaczorowski, J. Phys.: Condens. Matter **26**, 016004 (2014).
[19] S. Patil, S. K. Pandey, V. R. R. Medicherla, R. S. Singh, R. Bindu, E. V. Sampathkumaran, and K. Maiti, J. Phys.: Condens. Matter **22**, 255602 (2010).
[20] S. Patil, V. R. R. Medicherla, R. S. Singh, E. V. Sampathkumaran, and K. Maiti, Europhys. Lett. **97**, 17004 (2012).
[21] G. Panaccione *et al*., Rev. Sci. Instrum. **80**, 043105 (2009).
[22] K. Koepernik and H. Eschrig, Phys. Rev. B **59**, 1743 (1999); I. Opahle, K. Koepernik, and H. Eschrig, *ibid*. **60**, 14035 (1999).
[23] J. P. Perdew and Y. Wang, Phys. Rev. B **45**, 13244 (1992); D. M. Ceperley and B. J. Alder, Phys. Rev. Lett. **45**, 566 (1980).
[24] V. I. Anisimov, I. V. Solovyev, M. A. Korotin, M. T. Czyżyk, and G. A. Sawatzky, Phys. Rev. B **48**, 16929 (1993).
[25] J. J. Yeh and I. Lindau, At. Data Nucl. Data Tables **32**, 1 (1985).
[26] S. Hüfner, *Photoelectron Spectroscopy* (Springer, Berlin, 1993).
[27] A. Zangwill, *Physics at Surfaces* (Cambridge University Press, Cambridge, 1988).
[28] Y. Iwamoto *et al*., J. Phys.: Condens. Matter **7**, 1149 (1995).